



Providing Choice & Value

Generic CT and MRI Contrast Agents



**FRESENIUS
KABI**

CONTACT REP

AJNR






This information is current as
of July 18, 2025.

**Differentiating Low-Grade from High-Grade
Intracranial Ependymomas: Comparison of
Dynamic Contrast-Enhanced MRI and
Diffusion-Weighted Imaging**

Julio Arevalo-Perez, Elena Yllera-Contreras, Kyung K.
Peck, Vaios Hatzoglou, Onur Yildirim, Marc K. Rosenblum
and Andrei I. Holodny

AJNR Am J Neuroradiol published online 23 May 2024
<http://www.ajnr.org/content/early/2024/05/23/ajnr.A8226>

Differentiating Low-Grade from High-Grade Intracranial Ependymomas: Comparison of Dynamic Contrast-Enhanced MRI and Diffusion-Weighted Imaging

 Julio Arevalo-Perez,  Elena Yllera-Contreras,  Kyung K. Peck, Vaivos Hatzoglou,  Onur Yildirim, Marc K. Rosenblum, and  Andrei I. Holodny

ABSTRACT

BACKGROUND AND PURPOSE: The aim of this study was to determine the diagnostic value of fractional plasma volume derived from dynamic contrast-enhanced perfusion MR imaging versus ADC, obtained from DWI in differentiating between grade 2 (low-grade) and grade 3 (high-grade) intracranial ependymomas.

MATERIALS AND METHODS: A hospital database was created for the period from January 2013 through June 2022, including patients with histologically-proved ependymoma diagnosis with available dynamic contrast-enhanced MR imaging. Both dynamic contrast-enhanced perfusion and DWI were performed on each patient using 1.5T and 3T scanners. Fractional plasma volume maps and ADC maps were calculated. ROIs were defined by a senior neuroradiologist manually by including the enhancing tumor on every section and conforming a VOI to obtain the maximum value of fractional plasma volume ($V_{p_{max}}$) and the minimum value of ADC (ADC_{min}). A Mann-Whitney U test at a significance level of corrected $P = .01$ was used to evaluate the differences. Additionally, receiver operating characteristic curve analysis was applied to assess the sensitivity and specificity of $V_{p_{max}}$ and ADC_{min} values.

RESULTS: A total of 20 patients with ependymomas (10 grade 2 tumors and 10 grade 3 tumors) were included. $V_{p_{max}}$ values for grade 3 ependymomas were significantly higher ($P < .002$) than those for grade 2. ADC_{min} values were overall lower in high-grade lesions. However, no statistically significant differences were found ($P = .12114$).

CONCLUSIONS: As a dynamic contrast-enhanced perfusion MR imaging metric, fractional plasma volume can be used as an indicator to differentiate grade 2 and grade 3 ependymomas. Dynamic contrast-enhanced perfusion MR imaging plays an important role with high diagnostic value in differentiating low- and high-grade ependymoma.

ABBREVIATIONS: ADC_{min} = minimum ADC; AIF = arterial input function; AUC = area under the curve; DCE = dynamic contrast-enhanced; rCBV = relative CBV; ROC = receiver operating characteristic; VEGF = vascular endothelial growth factor; $V_{p_{max}}$ = maximum plasma volume; V_p = fractional plasma volume; WHO = World Health Organization

Intracranial ependymomas are a heterogeneous group of glial cell tumors of the CNS that arise from the ependymal lining of the ventricles, cerebral hemispheres, and central canal of the spinal cord. Intracranial ependymomas are uncommon primary neoplasms, accounting for 2.5% of all intracranial gliomas and 7% of primary CNS malignancies diagnosed annually.¹ They

account for 1%–3% of brain tumors in adults and 5%–12% in children.^{1,2}

Categorization of these tumors is essential because their treatment and prognosis vary. In 2016, the World Health Organization (WHO) classified ependymomas as low-grade (grade 2) and anaplastic ependymomas as high-grade (grade 3).^{2,3} Surgery is the primary treatment in both pediatric and adult populations. In patients with low-grade tumors, close surveillance can be sufficient, provided there has been complete resection. In contrast, patients with high-grade ependymoma need postoperative radiation therapy after gross total resection.^{3–6} Additionally, high-grade ependymomas have a poorer prognosis. Five-year overall survival and 2-year progression-free survival rates are 30% and 20%, respectively, compared with 100% and 77.8% for their low-grade counterparts.³ Consequently, preoperative classification of ependymomas is crucial for tailored management and risk stratification. Unfortunately, imaging findings on conventional MR imaging and

Received December 19, 2023; accepted after revision February 7, 2024.

From the Departments of Radiology (J.A.-P., E.Y.-C., V.H., O.Y., A.I.H.), Medical Physics (K.K.P.), and Pathology (M.K.R.), Memorial Sloan Kettering Cancer Center, New York, New York.

Drs Julio Arevalo-Perez and Elena Yllera-Contreras contributed equally to the work as coauthors.

This work was supported by the National Institutes of Health: NIH-NCI P30 CA008748 (Vickers, PI).

Please address correspondence to Julio Arevalo-Perez, MD, PhD., Memorial Sloan Kettering Cancer Center, Department of Radiology, 1275 York Ave, New York, NY, 10065-6007; e-mail: arevalj@mskcc.org

<http://dx.doi.org/10.3174/ajnr.A8226>

SUMMARY SECTION

PREVIOUS LITERATURE: Previous literature has shown that ADC values are different between high-grade and low-grade ependymomas, supporting the use of ADC as an objective and noninvasive marker for presurgical differentiation of low-grade and high-grade ependymomas. Other authors have also shown that perfusion marker relative CBV derived from DSC MR imaging was higher in high-grade ependymomas than those of low-grade tumors. These advanced techniques have also been compared showing lower relative ADC_{min} and higher relative CBV_{max} values among patients with high-grade ependymomas than with low-grade ependymomas. Based on the above findings we seek to compare DCE and ADC.

KEY FINDINGS: Vp_{max}, a surrogate marker of vascularization derived for DCE MR imaging, showed significant differences between ependymoma grades. ADC_{min} values differed also between high-grade and low-grade ependymomas but no statistically significant differences were found, implying that Vp_{max} is a better discriminator of ependymoma grade.

KNOWLEDGE ADVANCEMENT: Because Vp_{max}, derived from DCE MR imaging, less susceptible to artifacts than DSC, is superior to ADC_{min} in the classification of ependymomas according to grades, the inclusion of fractional plasma volume (Vp) perfusion maps in the standard MR imaging of primary brain tumors could represent an improved added diagnostic value and help in treatment guidance.

clinical manifestations often overlap, making presurgical classification difficult to achieve.⁷

Conventional MR imaging is a noninvasive imaging technique that supports the diagnosis, surgical planning, clinical management, and assessment of the treatment response of brain tumors. Despite its utility, conventional MR imaging provides little information concerning the physiologic behavior of a tumor.⁸ In fact, it is complicated to differentiate low- and high-grade ependymomas solely on the basis of the enhancement pattern or morphologic features that conventional MR imaging provides. Advanced MR imaging techniques, such as MR imaging perfusion and DWI, have proved helpful for the assessment of tumor neovascularity and cellularity, as well as in grading tumors.^{9,10} Recently, a few attempts have been made to classify ependymomas from an imaging standpoint, including a comparison of DSC and ADC.^{3,7}

The objective of our study was to compare the differences of maximum plasma volume (Vp_{max}) derived from dynamic contrast-enhanced (DCE) MR imaging and minimum ADC (ADC_{min}) in differentiating grade 2 and 3 ependymomas. We hypothesized that Vp_{max}, derived from T1-weighted DCE-MR imaging perfusion, would outperform ADC_{min} in discriminating ependymoma grades.

MATERIALS AND METHODS

Patients, Imaging Protocol, and Statistical Analysis

This retrospective study was performed after local institutional review board approval, including a waiver of informed consent. A hospital database was created for the period from January 2013 through June 2022, including patients with a histologically-proved ependymoma diagnosis with available DCE-MR imaging.

MR Imaging Acquisition

MR imaging sequences were acquired via 1.5T (Optima 450W; GE Healthcare) and 3T (Signa Premier 750W; GE Healthcare) and a standard 8-channel head coil. A bolus of gadolinium-diethylenetriaminepentaacetic acid, Gadobutrol (Gadavist; Bayer), was administered via a power injector at 0.1 mmol/kg body weight and a rate of 2–3 mL/s via a venous catheter (18–21 ga). Kinetic enhancement of the tissue was obtained both during and after

injection of gadolinium-diethylenetriaminepentaacetic acid by using a 3D T1-weighted fast echo-spoiled gradient-echo sequence (TR = 4–5 ms; TE = 1–2 ms; section thickness = 5 mm; flip angle = 25°;^{11,12} FOV = 32 cm; temporal resolution = 5–6 seconds) and consisted of 32 images in the axial plane.

Matching contrast T1-weighted (TR/TE = 600/8 ms; thickness = 4.5 mm) and T2-weighted (TR/TE = 4000/102 ms; thickness = 4.5 mm) spin-echo images were obtained. The kinetic enhancement of tissue before, during, and after injection of gadolinium-diethylenetriaminepentaacetic acid was obtained by using a 3D T1-weighted fast-spoiled gradient-echo sequence (TR, 4–5 ms; TE, 1–2 ms; section thickness, 3 mm; flip angle, 25°; FOV, 24 cm; matrix, 128 × 128; temporal resolution, 5–6 seconds) and consisted of 10–12 images in the axial plane. Ten phases for preinjection time delay and 30 phases for postinjection were obtained. DCE matching post-T1-weighted images were additionally acquired after DCE-MR imaging.

DWI was performed in the axial plane using a spin-echo EPI sequence with the following parameters: TR/TE = 8000/104.2 ms; diffusion gradient encoding in 3 orthogonal directions; b = 1000 s/mm²; FOV = 240 mm; matrix size = 128 × 128 pixels; section thickness = 5 mm; section gap = 1 mm; and number of averages = 2. DWI scans were obtained before DCE-MR imaging. The ADC values were calculated as follows: $ADC = [\ln(S/S_0)]/b$, wherein S is the signal intensity of the ROI obtained through 3 orthogonally oriented DWIs or diffusion trace images, S₀ is the signal intensity of the ROI acquired through reference T2-weighted images, and b is the gradient b factor with a value of 1000 s/mm².² ADC maps were calculated on a pixel-by-pixel basis.

Image Analysis

We processed and analyzed DCE-MR perfusion imaging data using NordicICE (Version 4.2.0; NordicNeuroLab). Preprocessing steps included background noise removal, spatial and temporal smoothing, and detection of the arterial input function (AIF) from the MCA. AIF was individually computed, and AIF curves with a rapid increase in signal enhancement and sharp peak followed by minimal temporal noises were selected. We applied the extended Tofts 2-compartment pharmacokinetic model, which assumes that the contrast agent is either in the interstitial space

or in the intravascular compartment, to calculate the DCE-MR perfusion imaging parameter fractional plasma volume (V_p).¹³ A senior neuroradiologist with 15 years of experience manually delineated ROIs by including the enhancing tumor on every section and conforming a VOI, with careful consideration to exclude large vessels on each T1-weighted DCE-MR perfusion image. FuncTool software (AW5.2; GE Healthcare) was used for ADC map postprocessing. Because previous studies have found that maximal perfusion values and minimum ADC values are most accurate for tumor grading,^{9,14-19} the volumes were then transferred to V_p maps to obtain the maximum plasma volume value ($V_{p_{max}}$) and to ADC maps to obtain the ADC_{min} . A ratio of tumor to normal brain parenchyma was obtained in both parameters for normalization purposes by placing ROIs in healthy-appearing white/gray matter of the contralateral hemisphere over normal brain parenchyma.

Statistical Analysis

A Mann-Whitney U test at a significance level of corrected $P < .01$ was applied to evaluate ADC and DCE MR imaging differences across tumor grades. Additionally, receiver operating characteristic (ROC) curve analysis was used to assess the sensitivity and specificity of $V_{p_{max}}$ and ADC_{min} values. SPSS statistical software (SPSS Statistics for Windows, Version 27.0; IBM) was used to perform the ROC curve analysis.

RESULTS

Patient Population

Twenty patients (age range, 6–72 years; interquartile range, 41.75 years; mean, 35.2 [SD, 21.67] years) with the diagnosis of ependymoma and DCE-MR imaging perfusion scans were identified. They were classified according to tumor grade: 10 low-grade ependymomas (grade 2) (8 males [80%] and 2 females [20%]) and 10 high-grade ependymomas (grade 3) (6 females and 4 males [50%]). The Table and Fig 1 show examples of histopathologic findings for low-grade (A) and high-grade (B)

ependymoma. Figure 2 shows examples of T1-weighted post-contrast, plasma volume, and ADC maps of low- and high-grade ependymomas.

Quantitative Perfusion Analysis

Normalized $V_{p_{max}}$ values for high-grade (grade 3) ependymomas were significantly higher ($P = .00018$) than those for low-grade ependymomas (grade 2). A boxplot of normalized V_p and ADC between low- and high-grade ependymomas is shown in Fig 3. In high-grade ependymomas, the mean normalized $V_{p_{max}}$ was 14.95 (SD, 6.91). In the low-grade group, the mean normalized $V_{p_{max}}$ was 2.01 (SD, 0.76). Normalized ADC_{min} values were overall lower in high-grade lesions (mean, 0.76 [SD, 0.25]) compared with low-grade lesions (mean, 0.88 [SD, 0.078]). However, no statistically significant differences were found ($P = .14156$).

ROC Analysis

The ROC curve analysis was applied to evaluate the diagnostic value of the normalized $V_{p_{max}}$ and ADC_{min} values to differentiate high- and low-grade ependymomas. On the basis of the ROC analysis, normalized $V_{p_{max}}$ shows a sensitivity of 100% and specificity of 100% to differentiate high- and low-grade ependymomas (Fig 4). The area under the curve (AUC) for $V_{p_{max}}$ was the highest (AUC = 1), indicating a better classification ability in differentiating low- and high-grade ependymomas, compared with ADC_{min} (AUC = 0.29; asymptotic 95% CI, 0.05–0.53).

DISCUSSION

Our study demonstrated that $V_{p_{max}}$ was a superior discriminator over ADC_{min} between low- and high-grade ependymomas. Notably, the parameter $V_{p_{max}}$, a surrogate marker of vascularization, showed statistically significant differences, while ADC_{min} values showed no statistically significant differences despite variance between grades.

Perfusion imaging has been widely used in recent years to classify brain tumors.^{8,20} Extensive documentation can be found

Demographic data, location of tumor, field strength of scanner, and normalized $V_{p_{max}}$ and ADC_{min} values

Histopathology	Age	Location	Sex	Field Strength	rVP _{max}	rADC _{min}
Low-grade ependymoma	21	Posterior Fossa	M	3T	2.57	0.8
Low-grade ependymoma	72	Supratentorial	M	3T	0.95	1.02
Low-grade ependymoma	51	Posterior Fossa	F	3T	1.09	0.91
Low-grade ependymoma	70	Posterior Fossa	M	3T	1.8	0.9
Low-grade ependymoma	20	Posterior Fossa	M	3T	1.53	0.73
Low-grade ependymoma	57	Posterior Fossa	M	3T	2.75	0.85
Low-grade ependymoma	36	Posterior Fossa	M	3T	1.41	0.89
Low-grade ependymoma	58	Posterior Fossa	M	1.5T	2.98	0.93
Low-grade ependymoma	9	Supratentorial	F	3T	2.12	0.92
Low-grade ependymoma	13	Posterior Fossa	M	3T	2.93	0.85
Anaplastic ependymoma	16	Posterior Fossa	M	1.5T	16.29	0.73
Anaplastic ependymoma	14	Posterior Fossa	M	3T	21.56	0.79
Anaplastic ependymoma	59	Supratentorial	M	1.5T	5.43	0.29
Anaplastic ependymoma	29	Supratentorial	F	3T	23.19	0.53
Anaplastic ependymoma	32	Supratentorial	F	3T	11.11	0.9
Anaplastic ependymoma	58	Supratentorial	M	1.5T	7.07	1.15
Anaplastic ependymoma	6	Posterior Fossa	F	3T	21.9	0.99
Anaplastic ependymoma	42	Supratentorial	F	1.5T	22.5	0.83
Anaplastic ependymoma	10	Posterior Fossa	F	3T	10.04	0.51
Anaplastic ependymoma	31	Posterior Fossa	F	3T	10.4	0.83

Note:—rVP_{max} indicates relative maximum plasma volume, rADC_{min}, relative ADC_{min}.

in the literature about the correlation between perfusion imaging with conventional angiography of vascular density and histologic analysis of microvascular density, as well as the expression of vascular endothelial growth factor (VEGF).²¹⁻²⁶

High-grade ependymomas are aggressive and express more VEGF. Consequently, they are more proliferating with more

vascular invasion, which leads to insufficient tumor blood supply. Therefore, necrosis is more frequently seen in high-grade ependymomas than in low-grade ependymomas.²⁷ The assessment of ependymomas using perfusion imaging has been minimal. To our knowledge, only 1 prior study has attempted to classify ependymomas exclusively by using perfusion imaging. Xing et al³

used DSC-perfusion, an advanced MR imaging technique that uses relative CBV (rCBV) to evaluate the vascularity of brain tumors indirectly. Their study comprised 15 patients (11 with high-grade ependymoma and 4 with low-grade ependymoma) who underwent DSC perfusion. This was, to date, the largest reported cohort. In this cohort, the relative CBV_{max} values of high-grade ependymomas were higher than those of low-grade tumors, probably due to vascular proliferation in high-grade lesions. However, the cohort's low-grade ependymoma sample comprised a small

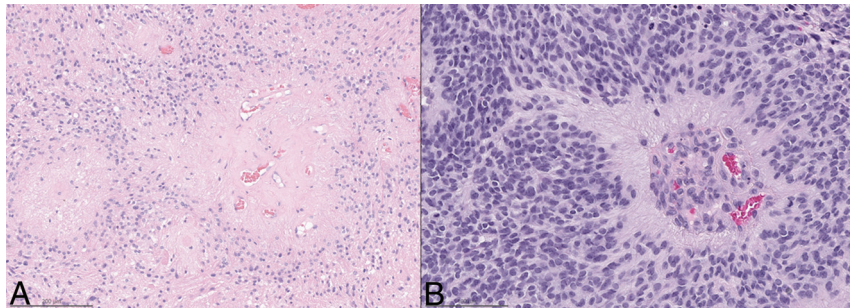


FIG 1. Histopathologic features of low-grade (A) and high-grade (B) ependymomas. A, Modestly cellular low-grade ependymoma, with broad perivascular pseudorosettes, devoid of mitotic activity. B, Densely cellular high-grade ependymoma, with a narrower perivascular pseudorosette, microvascular proliferation, and mitotic activity.

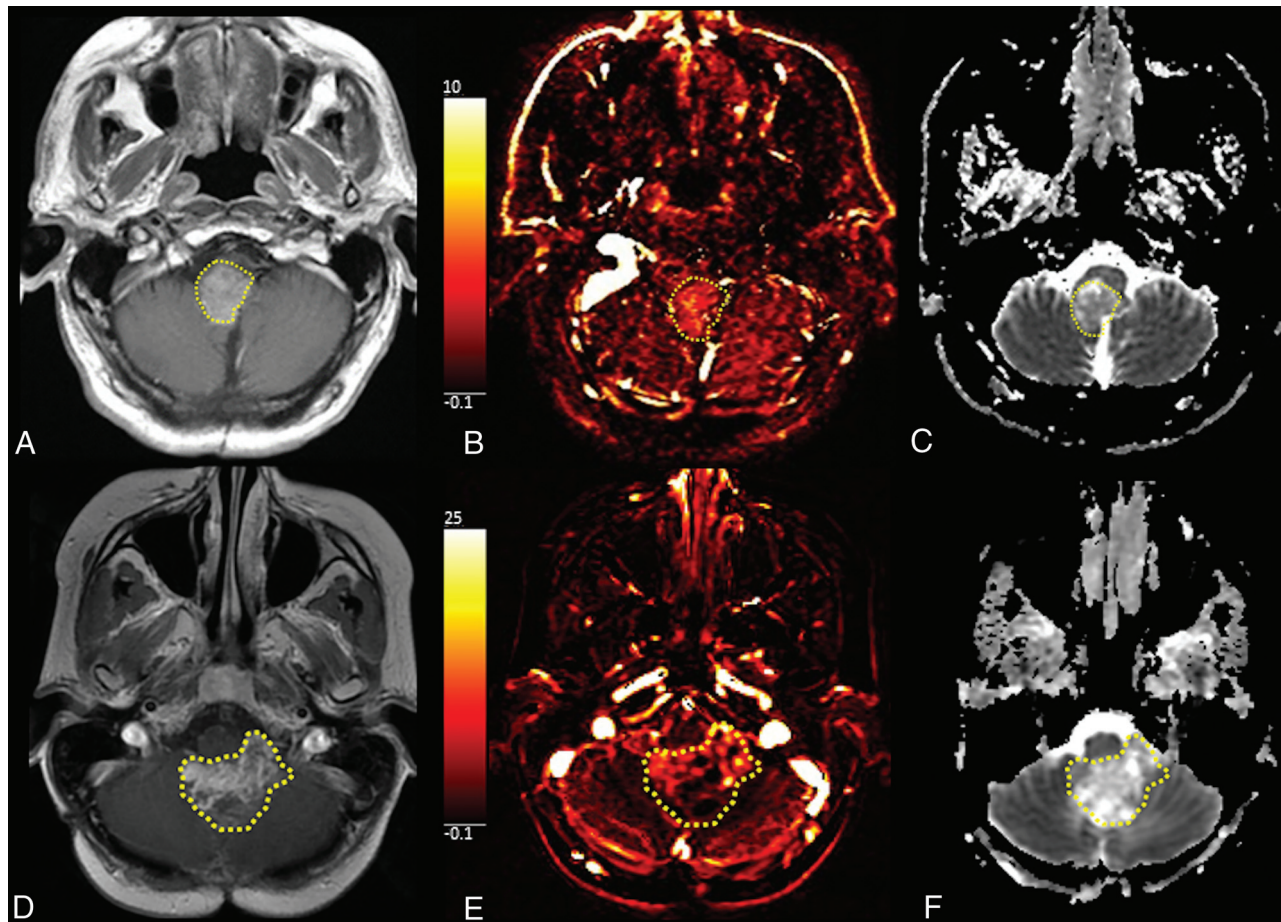


FIG 2. Examples of low-grade ependymomas (A, B, and C). A, T1-weighted postcontrast axial image demonstrates an enhancing mass in the inferior fourth ventricle and along the lower pons and dorsal medulla. B, Vp perfusion map shows mild elevation of Vp, 5.43. C, ADC map shows mildly elevated ADC values (579 mm²/s). Examples of high-grade ependymomas (D, E, and F). D, T1-weighted postcontrast axial image shows a heterogeneously enhancing partially cystic mass centered within the fourth ventricle with mass effect. E, Vp map shows areas of cystic changes and necrosis but also foci of elevated Vp (19.39), suggesting high vascularity. F, ADC map shows overall increased values with scattered areas of low ADC (514 mm²/s). The highlighted areas show the enhancing tumor in the inferior fourth ventricle; low-grade ependymoma, images A, B and C and high-grade ependymoma, images D, E and F.

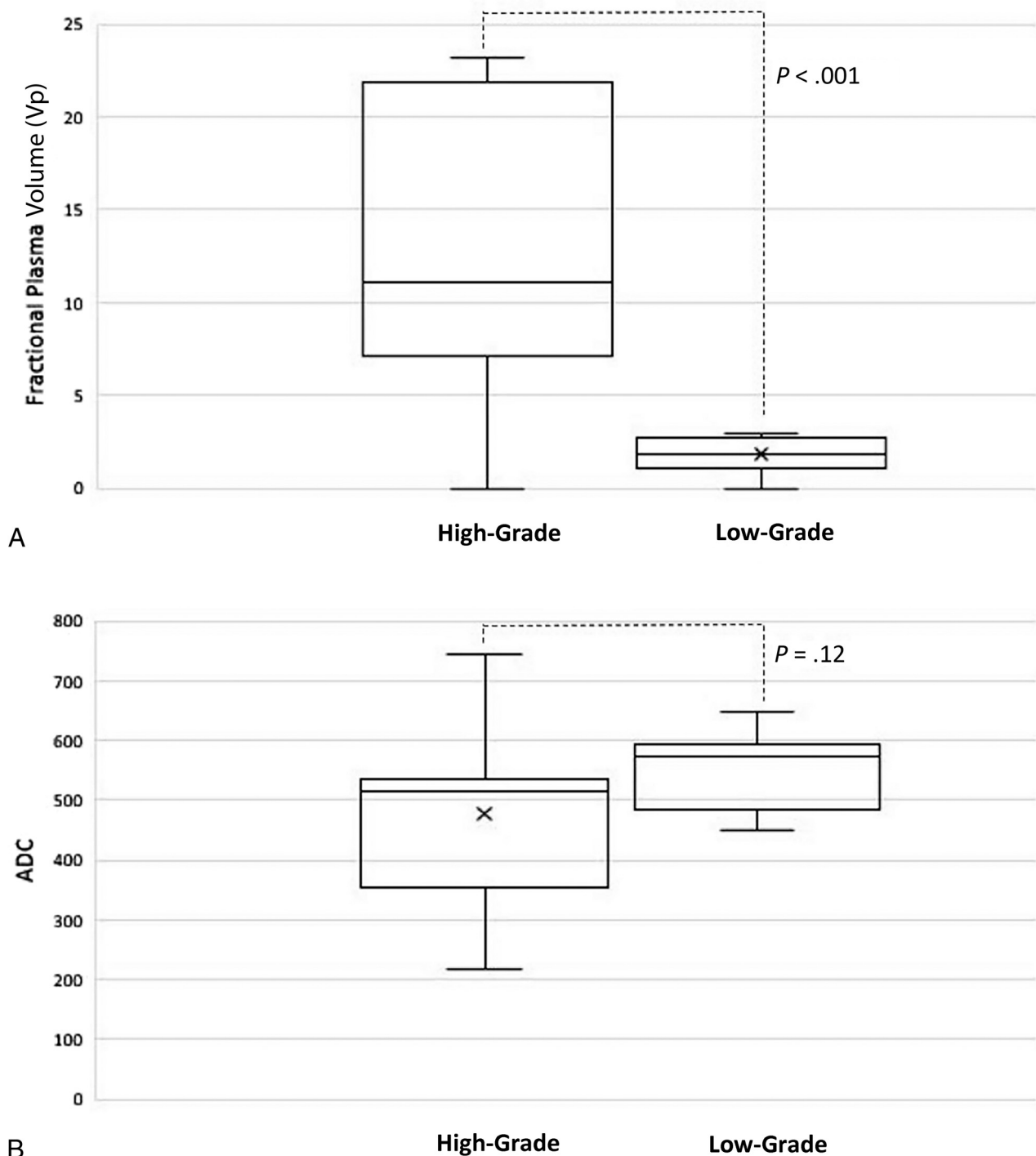


FIG 3. Boxplot of normalized Vp and ADC between low-grade and high-grade ependymomas.

number of patients, and their conclusions should consequently be interpreted cautiously.³ Additionally, it is known that rCBV values obtained from DSC are a semiquantitative measurement, which can be influenced by several postprocessing phases, including a correction technique, to address contrast extravasation and the choice of normal contralateral white matter.^{28,29} DSC perfusion imaging is also exquisitely sensitive to susceptibility artifacts. It can easily be affected by calcification, hemorrhage, and bone and has a potentially biased measurement

due to T1 effects from extravascular contrast leakage in tumor vasculature.³⁰

In our study, we used DCE-MR imaging, a T1-weighted perfusion method that is less sensitive to susceptibility artifacts than DSC in estimating absolute CBV. We used Vp, a pharmacokinetic parameter derived from DCE-MR imaging that is similar to the physiologic meaning of rCBV calculated from DSC. However, Hacklander et al³¹ demonstrated that Vp was superior to rCBV for quantitative estimation of CBV because

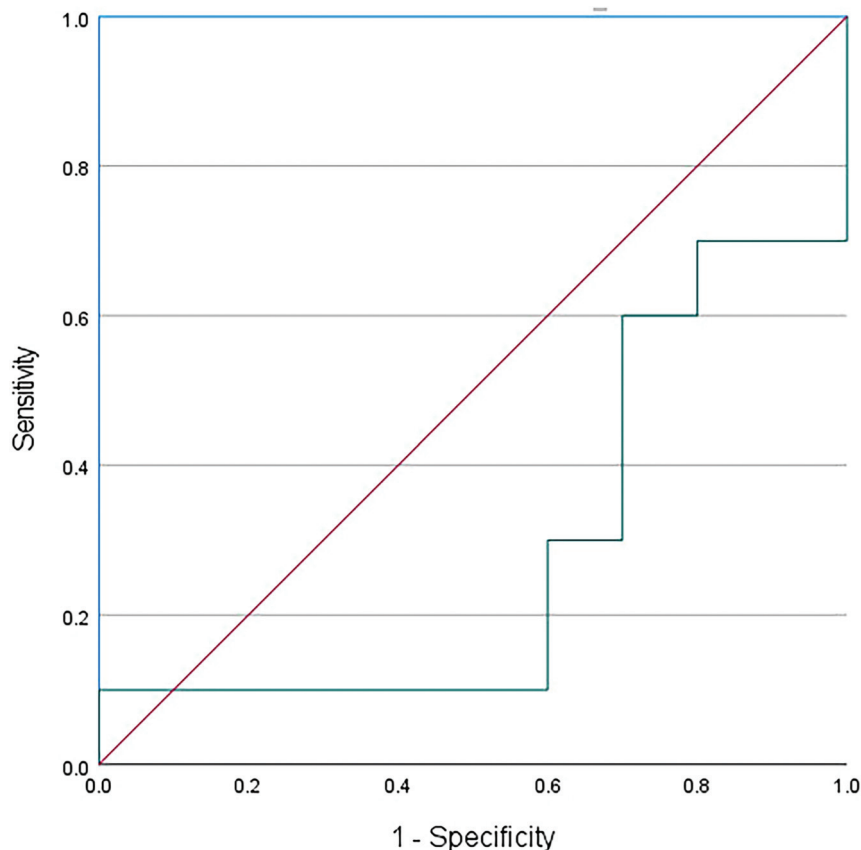


FIG 4. ROC curve of Vp (blue) and ADC (green) values to differentiate low- and high-grade of ependymoma (reference line: red).

it is based on T1-weighted perfusion and is less prone to artifacts. Our patient cohort comprised 20 histologically confirmed cases and had a well-balanced ratio of high-grade-to-low-grade tumors (10:10). Also, ROC curve analysis showed that Vp_{max} has a sensitivity and specificity of 100%. We realize, however, that MR imaging characteristics are very rarely if ever 100% sensitive and specific. Our, perhaps overly optimistic, results are probably due to the small sample size.

DWI is a functional MR imaging technique that measures the random motion of water molecules within a tissue volume. ADC maps, derived from DWI, show the reduction of the mobility of water molecules due to high cellularity or cellular swelling. In the context of tumor characterization, a decrease in ADC values suggests higher cellularity and, therefore, a higher tumor grade.⁹ This principle has been used in the literature to characterize different tumors, but only 1 study has addressed the classification of ependymomas by using ADC.⁷ In their study, Xianwang et al⁷ found that ADC_{mean} values of adult intracranial ependymomas were higher than those of high-grade ependymomas, supporting the use of ADC as an objective and noninvasive marker for presurgical differentiation of low- and high-grade ependymomas. They analyzed 20 low-grade and 15 high-grade ependymomas, all with histologic confirmation. Additionally, they provided the Ki-67 proliferation index of each patient's tumor tissue.

Xing et al³ compared conventional MR imaging, DWI, and DSC-PWI to show lower relative ADC_{min} and higher relative

CBV_{max} values among patients with high-grade extraventricular ependymomas than those with low-grade ependymomas. This finding may be attributable to the high proportion of cellularity and vascular proliferation in high-grade ependymomas. Prior studies have shown that analysis of entire tumor volume, including possibly cystic and necrotic areas, could influence ADC measurements by increasing the ADC values.^{9,32} Necrosis and cystic changes are more frequently found in high-grade tumors, which could represent a confounding factor when attempting tumor classification via ADC_{mean} alone. Instead, we used ADC_{min} , which showed that high-grade ependymomas had lower ADC values than in the low-grade group. However, no statistically significant differences were found, possibly explained by the smaller sample size.

One of the main limitations of our study was its small sample size (20 patients with histologically-proved ependymomas). Many patients are referred to our highly specialized oncologic care center for a second opinion in therapeutic management after the initial resection of their tumor at another institution. It

is, therefore, challenging for us to find unresected, treatment-naïve primary brain tumors. Our study span intersected with the release of the updated WHO classification in 2021; therefore, all tumors were classified according to the WHO classifications of 2007 and 2016, considering only histologic features. Consequently, the absence of a correlation between patient immunohistochemical characteristics is an additional limitation, which could offer supplementary insight into prognostic, genetic, and predictive information. Finally, the manual method by which tumor volumes were extracted and calculated could represent another limitation. However, we tried to mitigate the reproducibility bias by having a single trained operator perform all VOIs.

CONCLUSIONS

DCE perfusion MR imaging and plasma volume parameters in particular perform better than ADC in noninvasive differentiation of grade 2 and grade 3 ependymomas. Including DCE perfusion maps in the standard MR imaging of primary brain tumors can help to improve diagnostic value and treatment guidance.

Disclosure forms provided by the authors are available with the full text and PDF of this article at www.ajnr.org.

REFERENCES

1. Lombardi G, Della Puppa A, Pizzi M, et al. **An overview of intracranial ependymomas in adults.** *Cancers (Basel)* 2021;13:6128 [CrossRef](#) [Medline](#)

2. Louis DN, Perry A, Reifenberger G, et al. **The 2016 World Health Organization Classification of Tumors of the Central Nervous System: a summary.** *Acta Neuropathol* 2016;131:803–20 [CrossRef Medline](#)
3. Xing Z, Zhou X, Xiao Z, et al. **Comparison of conventional, diffusion, and perfusion MRI between low-grade and anaplastic extraventricular ependymoma.** *AJR Am J Roentgenol* 2020;215:978–84 [CrossRef Medline](#)
4. Shuangshoti S, Rushing EJ, Mena H, et al. **Supratentorial extraventricular ependymal neoplasms: a clinicopathologic study of 32 patients.** *Cancer* 2005;103:2598–605 [CrossRef Medline](#)
5. Sun S, Wang J, Zhu M, et al. **Clinical, radiological, and histological features and treatment outcomes of supratentorial extraventricular ependymoma: 14 cases from a single center.** *J Neurosurg* 2018;128:1396–402 [CrossRef Medline](#)
6. Oya N, Shibamoto Y, Nagata Y, et al. **Postoperative radiotherapy for intracranial ependymoma: analysis of prognostic factors and patterns of failure.** *J Neurooncol* 2002;56:87–94 [CrossRef Medline](#)
7. Xianwang L, Lei H, Hong L, et al. **Apparent diffusion coefficient to evaluate adult intracranial ependymomas: relationship to Ki-67 proliferation index.** *J Neuroimaging* 2021;31:132–36 [CrossRef Medline](#)
8. Gupta PK, Saini J, Sahoo P, et al. **Role of dynamic contrast-enhanced perfusion magnetic resonance imaging in grading of pediatric brain tumors on 3T.** *Pediatr Neurosurg* 2017;52:298–305 [CrossRef Medline](#)
9. Arevalo-Perez J, Peck KK, Young RJ, et al. **Dynamic contrast-enhanced perfusion MRI and diffusion-weighted imaging in grading of gliomas.** *J Neuroimaging* 2015;25:792–98 [CrossRef Medline](#)
10. Vajapeyam S, Brown D, Johnston PR, et al. **Multiparametric analysis of permeability and ADC histogram metrics for classification of pediatric brain tumors by tumor grade.** *AJNR Am J Neuroradiol* 2018;39:552–57 [CrossRef Medline](#)
11. Nam JG, Kang KM, Choi SH, et al. **Comparison between the prebolus T1 measurement and the fixed T1 value in dynamic contrast-enhanced MR imaging for the differentiation of true progression from pseudoprogression in glioblastoma treated with concurrent radiation therapy and temozolomide chemotherapy.** *AJNR Am J Neuroradiol* 2017;38:2243–50 [CrossRef Medline](#)
12. Conte GM, Altabella L, Castellano A, et al. **Comparison of T1 mapping and fixed T1 method for dynamic contrast-enhanced MRI perfusion in brain gliomas.** *Eur Radiol* 2019;29:3467–79 [CrossRef Medline](#)
13. Tofts PS, Brix G, Buckley DL, et al. **Estimating kinetic parameters from dynamic contrast-enhanced T(1)-weighted MRI of a diffusable tracer: standardized quantities and symbols.** *J Magn Reson Imaging* 1999;10:223–32 [CrossRef Medline](#)
14. Hilario A, Ramos A, Perez-Nunez A, et al. **The added value of apparent diffusion coefficient to cerebral blood volume in the preoperative grading of diffuse gliomas.** *AJNR Am J Neuroradiol* 2012;33:701–07 [CrossRef Medline](#)
15. Santarosa C, Castellano A, Conte GM, et al. **Dynamic contrast-enhanced and dynamic susceptibility contrast perfusion MR imaging for glioma grading: preliminary comparison of vessel compartment and permeability parameters using hotspot and histogram analysis.** *Eur J Radiology* 2016;85:1147–56 [CrossRef Medline](#)
16. Calli C, Kitis O, Yuntun N, et al. **Perfusion and diffusion MR imaging in enhancing malignant cerebral tumors.** *Eur J Radiol* 2006;58:394–403 [CrossRef Medline](#)
17. Kono K, Inoue Y, Nakayama K, et al. **The role of diffusion-weighted imaging in patients with brain tumors.** *AJNR Am J Neuroradiol* 2001;22:1081–88 [Medline](#)
18. Lee EJ, Lee SK, Agid R, et al. **Preoperative grading of presumptive low-grade astrocytomas on MR imaging: diagnostic value of minimum apparent diffusion coefficient.** *AJNR Am J Neuroradiol* 2008;29:1872–77 [CrossRef Medline](#)
19. Kim HS, Kim SY. **A prospective study on the added value of pulsed arterial spin-labeling and apparent diffusion coefficients in the grading of gliomas.** *AJNR Am J Neuroradiol* 2007;28:1693–99 [CrossRef Medline](#)
20. Vajapeyam S, Stamoulis C, Ricci K, et al. **Automated processing of dynamic contrast-enhanced MRI: correlation of advanced pharmacokinetic metrics with tumor grade in pediatric brain tumors.** *AJNR Am J Neuroradiol* 2017;38:170–75 [CrossRef Medline](#)
21. Cha S, Johnson G, Wadghiri YZ, et al. **Dynamic, contrast-enhanced perfusion MRI in mouse gliomas: correlation with histopathology.** *Magn Reson Med* 2003;49:848–55 [CrossRef Medline](#)
22. Maia AC, Jr., Malheiros SM, da Rocha AJ, et al. **MR cerebral blood volume maps correlated with vascular endothelial growth factor expression and tumor grade in nonenhancing gliomas.** *AJNR Am J Neuroradiol* 2005;26:777–83 [Medline](#)
23. Aronen HJ, Gazit IE, Louis DN, et al. **Cerebral blood volume maps of gliomas: comparison with tumor grade and histologic findings.** *Radiology* 1994;191:41–51 [CrossRef Medline](#)
24. Aronen HJ, Pardo FS, Kennedy DN, et al. **High microvascular blood volume is associated with high glucose uptake and tumor angiogenesis in human gliomas.** *Clin Cancer Res* 2000;6:2189–200 [Medline](#)
25. Sugahara T, Korogi Y, Kochi M, et al. **Correlation of MR imaging-determined cerebral blood volume maps with histologic and angiographic determination of vascularity of gliomas.** *AJR Am J Roentgenol* 1998;171:1479–86 [CrossRef Medline](#)
26. Arevalo-Perez J, Kebede AA, Peck KK, et al. **Dynamic contrast-enhanced MRI in low-grade versus anaplastic oligodendrogliomas.** *J Neuroimaging* 2016;26:366–71 [CrossRef Medline](#)
27. Wu J, Armstrong TS, Gilbert MR. **Biology and management of ependymomas.** *Neuro Oncol* 2016;18:902–13 [CrossRef Medline](#)
28. Ellingson BM, Zaw T, Cloughesy TF, et al. **Comparison between intensity normalization techniques for dynamic susceptibility contrast (DSC)-MRI estimates of cerebral blood volume (CBV) in human gliomas.** *J Magn Reson Imaging* 2012;35:1472–77 [CrossRef Medline](#)
29. Boxerman JL, Schmainda KM, Weisskoff RM. **Relative cerebral blood volume maps corrected for contrast agent extravasation significantly correlate with glioma tumor grade, whereas uncorrected maps do not.** *AJNR Am J Neuroradiol* 2006;27:859–67 [Medline](#)
30. Boxerman JL, Prah DE, Paulson ES, et al. **The role of preload and leakage correction in gadolinium-based cerebral blood volume estimation determined by comparison with MION as a criterion standard.** *AJNR Am J Neuroradiol* 2012;33:1081–87 [CrossRef Medline](#)
31. Hacklander T, Reichenbach JR, Modder U. **Comparison of cerebral blood volume measurements using the T1 and T2* methods in normal human brains and brain tumors.** *J Comput Assist Tomogr* 1997;21:857–66 [CrossRef Medline](#)
32. Lee J, Choi SH, Kim JH, et al. **Glioma grading using apparent diffusion coefficient map: application of histogram analysis based on automatic segmentation.** *NMR Biomed* 2014;27:1046–52 [CrossRef Medline](#)